Transpiration Cooling for Reusable Heat Shields During Earth Reentry

Curt Carman*, Cameron Entremont†, Joseph Harris‡, Jeremiah Clermont§
Mississippi State University, Mississippi State, MS 39759

To assess the feasibility of transpiration cooling on a heat shield, a preliminary study on the heating of a reentry capsule in simulated hypersonic flow has been accomplished. An ideal heat shield material, ultra-high-temperature ceramic (UHTC) zirconium diboride (ZrB_2), and coolant fluid of helium have been selected due to a literature review. Resulting from the availability of physical and experimental information for comparison, the Orion capsule was chosen for modeling in SOLIDWORKS and simulation in Ansys. Two main simulations were produced: one to gauge heating on the uncooled Orion capsule geometry in Mach 30 flow, and another to gauge the transpiration cooling effect on a flat plate with a coolant inlet. The simulations are intended to be combined to show transpiration cooling effectiveness on a heat shield. In Mach 30 flow, initial results from the raw Orion capsule geometry simulation reveal peak temperatures of 14,900 K in front of the heat shield, with results supported by analytical normal shock calculations. The higher-fidelity flat-plate transpiration cooling simulation at the heat shield's stagnation point reveals the potential for the cooling method to significantly reduce heating on the outer surface, though current modeling of the porous wall with a uniform mass flux has shown cooling effectiveness greater than realistically expected. This will be improved in the future by implementing pressure-driven porous media modeling rather than a prescribed uniform mass flux, extending the computational domain to reduce boundary effects, refining near-wall mesh resolution to better capture boundary layer transport, and incorporating a structural thermal model to accurately derive skin temperatures from the Orion model for inclusion in the transpiration cooling model.

Nomenclature

A	=	area
C	=	heat capacity
c_p	=	specific heat capacity
F	=	injection rate/blowing ratio
k	=	thermal conductivity
T	=	temperature
t	=	thickness
L	=	length
M	=	Mach number
$\dot{m}$	=	coolant mass flux
R	=	nose radius
R_a	=	gas constant for dry air[1]
Re_∞	=	Reynolds number
S	=	curve length from the stagnation point
u_f	=	coolant velocity
u_g	=	post-shock gas velocity
Y_{O2}	=	oxygen species mass fraction

* Undergraduate Senior, ASE Department, AIAA University Student Member 1745152
† Undergraduate Senior, ASE Department, AIAA University Student Member 1923120
‡ Undergraduate Senior, ASE Department, AIAA University Student Member 1774316
§ Undergraduate Senior, ASE Department, AIAA University Student Member 1923121

Y_N	=	nitrogen species mass fraction
Y_{N2}	=	diatomic nitrogen species mass fraction
α	=	angle of attack
γ	=	specific heats ratio
ε	=	emissivity
η	=	cooling effectiveness
ρ	=	density
ρ_f	=	coolant density
ρ_g	=	post-shock gas density
ϕ	=	porosity

I. Introduction

HEAT shields are a vital component for any space mission involving Earth reentry. As implied by the name, they protect the vehicle from the extreme heat resulting from hypersonic flow. Failure of such a critical element can directly lead to the loss of the payload within the return capsule, which is human life in some cases. To reduce the maximum temperature induced on a surface in hypersonic flow, there exist many different cooling techniques. Common techniques include ablatives, regenerative cooling, film cooling, and transpiration cooling. Ablatives temporarily serve as heat protection in the form of an additional coating applied to the heated surface, prior to reentry. When reentry occurs, the coating absorbs the heat and falls away, removing heat energy from the system [1]. This manner of cooling does not lend itself to reuse, as a reusable heat shield will have lower allowable temperatures and must return in similar condition. For this reason, active cooling methods which might usually be too complex are considered for reusable applications. A common form of active cooling, regenerative cooling, involves the use of a fluid coolant inside the heated surface, soaking in thermal energy. This type of cooling is commonly seen in rocket engine combustion chambers, where liquid propellant is circulated inside the engine walls prior to usage, reducing the heat of the engine while enhancing its performance. Heat shield regenerative cooling would involve the circulation of a fluid coolant inside the heat shield before being discarded [2]. Film cooling involves aspects of both ablatives and regenerative cooling; coolant fluid is transported from an inner layer of the heated surface to the heated surface itself by means of small, discrete perforations. The coolant soaks up heat while being transported to the surface, while also providing an additional layer of protection in front of the heated surface once discarded [3].

Transpiration cooling, the cooling method of interest, is very similar to film cooling. The difference lies in the method of transportation used for the coolant fluid to reach the heated surface. Instead of intentionally machined slots, the heated surface material is densely porous, so that the coolant fluid can be pumped through the surface, seeping to the outside along the entire surface area, comparable to the idea of sweating. Coolant evaporation removes additional thermal energy from the system as it is transported and discarded, allowing for lower temperatures along the heated surface. Additionally, the coolant does not need to be recirculated and cooled down. Common coolants used in this cooling technique include water, helium, nitrogen, and hydrogen.

Atmospheric reentry for a capsule can reach Mach 40 depending on the context of the corresponding space mission. Orion, the heat shield capsule modeled for the transpiration cooling study, reentered the atmosphere at Mach 32 on its return from the Artemis I lunar mission [4]. In hypersonic testing, airspeeds of this magnitude are very difficult to recreate for experimental purposes. Additionally, Mississippi State University does not possess a functioning hypersonic wind tunnel, limiting experimentation to only significantly lower speeds than expected. Since an experimental approach to the study would not yield many valuable results, a numerical approach was taken instead. Using simulations to predict thermal behavior provides a feasible, cost-effective way to replicate known results for the Orion capsule to validate the model and implement other flow data that was previously unknown. Upon validation, a simulation allows for an easier study of transpiration cooling, enabling future studies to proceed at a lower cost.

The remainder of this paper is organized as follows: Section 2 presents discussion and results, Section 3 discusses future work, and Section 4 provides a conclusion.

II. Discussion and Results

A. Material and Coolant Selection

The selection of the heat shield material is a crucial step in the design and analysis of thermal protection systems (TPSs). Materials used in hypersonic flight can be broadly classified into three groups: ceramics, composites, and refractory metals [5]. Requirements for hypersonic TPS materials include local aerothermodynamic criteria regarding high-temperature strength, thermal conductivity, heat capacity, melting temperature, and lightweight [5]. For transpiration cooling, a highly porous material is required to allow the coolant fluid to flow through. Ceramic-matrix-composites (CMCs) have the potential to be an excellent TPS material. There are multiple ongoing developments employing CMC materials specifically for reusable reentry vehicles like the X-38 [6]. Highly effective materials that have been previously used on thermal protection systems are thermal insulation tiles. Thermal insulation tiles are highly lightweight and are typically used on the windward surfaces of heat shields [7]. These tiles are designed to effectively radiate the absorbed heat back into the surrounding environment and withstand aerodynamic forces [7]. Ultra-high-temperature ceramics (UHTCs) are another excellent candidate for thermal protection systems. These materials offer high melting points and the ability to manufacture complex pore and channel arrangements [8]. The UHTC zirconium diboride (ZrB_2) was selected as the ideal transpiration cooling material due to its very high melting temperature (3505 K), porosity, and material properties [8]. The material properties of ZrB_2 are provided below in Table 1.

Table 1. Material properties of UHTC zirconium diboride [8, 9].

porosity, ϕ	0.42
emissivity, ε	0.7
thermal conductivity, k	41.4 W/m-K
density, ρ	6100 kg/m^3
specific heat capacity, c_p	437 J/kg-K

The coolant selection process for transpiration cooling began with analyzing and reading academic literature on previous research and reviewing the heat capacities of different coolants. Table 2 shows the heat capacities of five different coolant streams at a constant injection rate/blowing ratio of F = 1.0% [10]. The blowing ratio is a commonly used parameter to describe transpiration-cooling; it is the ratio of coolant transpired through the wall and the main flow after the bow shock [9]. Equation (1) is the formula that defines the blowing ratio, and the mass flux of the coolant can be calculated from a known blowing ratio. The heat capacity values were calculated by Liu et al. [10] using analytical and experimental methods for transpiration cooling.

Table 2. Heat capacities of the five coolant streams [10].

Coolant	Heat capacities, C (mJ/s-K)
Air	140.20
N_2	143.86
He	688.90
Ar	71.20
CO_2	116.80

$$F = \frac{\rho_f u_f}{\rho_g u_g} = \frac{\dot{m}}{\rho_g u_g} \tag{1}$$

Helium had the maximum heat capacity by far, thus resulting in the best cooling effectiveness by absorbing the most energy from the system [10]. An analysis was also conducted by the research paper on the effectiveness of the various coolants at different locations along the nose cone [10]. The ratio, S/R, is the curve length from the stagnation point over the nose radius [10]. The results of the analysis are shown below in Fig. 1.

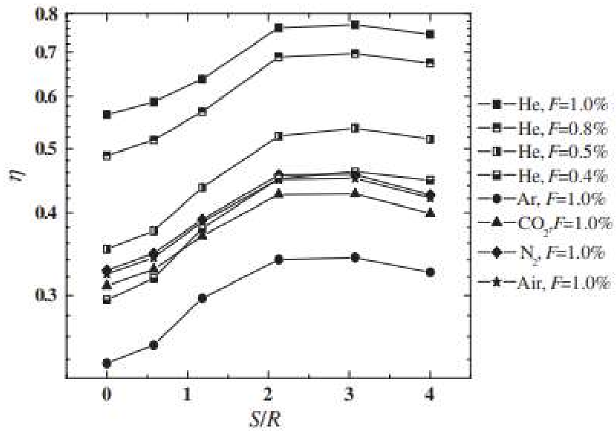

Figure 1. Cooling effectiveness for various coolants [10].
All the tests in this study are performed at T_∞ = 425 K and Re_∞ = 10^4.

Overall, helium consistently had the highest coolant effectiveness at different injection rates at the stagnation point and along the curve of the geometry. Based on these results, helium is by far the most effective coolant to use in transpiration cooling applications.

B. Computational Modeling

The immense difficulty of analytically solving or recreating the high-enthalpy hypersonic flows in wind tunnels points to the use of computational methods for simulating reentry phenomena. At these speeds, the immense kinetic energy is rapidly converted to thermal energy, creating strong bow shocks that can cause temperatures to reach high enough to trigger real gas effects. In these conditions, the fluid's density cannot be considered constant, and the vibrational excitation of the fluid causes its specific heat to vary with temperature. Thus, the fluid is said to be "calorically imperfect." Increasing Mach number and temperature further causes dissociation of air into oxygen and nitrogen, as the excess temperature goes towards breaking the fluid's chemical bonds. At this point, the fluid is considered thermally imperfect and no longer follows the equation of state. With increasing speed and temperature, the electrons are stripped from the oxygen and nitrogen, creating an ionized mixture [11]. The no-slip condition also may not be entirely accurate under these conditions, based on the scale of the vehicle.

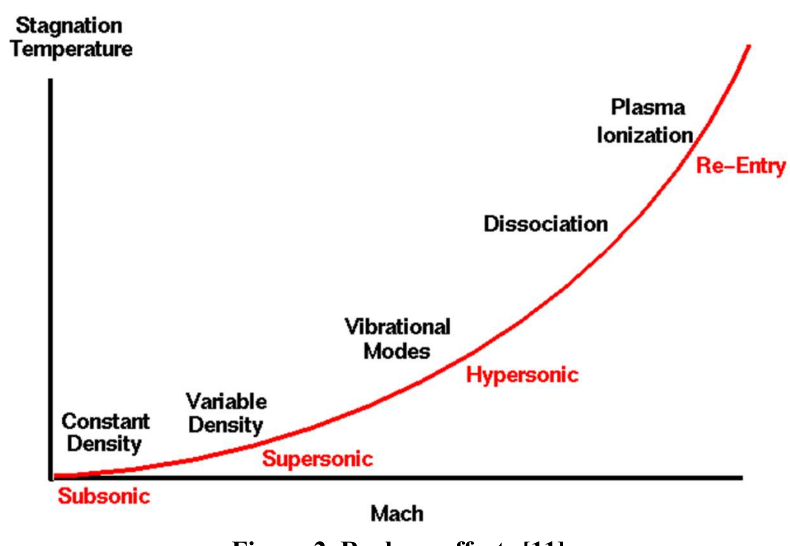

Figure 2. Real gas effects [11].

All these factors contribute to difficulties with modeling reentry dynamics and warrant the use of models that increase in complexity until accurate conditions are achieved. This also means that transpiration cooling should only be introduced into an already well-defined solution. For this reason, initial CFD simulations have been run with increasing complexity in a 2D domain, attempting to recreate reported values from the first flights of the Orion capsule before combining this model with a model of transpiration cooling over a flat plate.

1. Orion Capsule

The two-dimensional geometry of the Orion capsule is shown in Fig. 3, and the initial fluid domain used in the simulation is shown in Fig. 4. The initial domain was drawn as a rectangle with a large enough distance from the capsule to each boundary to allow the flow to exit the domain at farfield conditions, and Orion's geometry was cut out of the center.

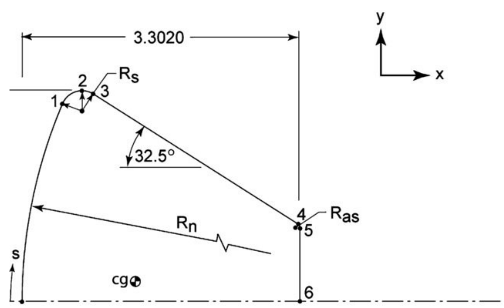

Location	x	y	s
1	0.4812	2.3615	2.4264
2	0.7126	2.5146	2.7203
3	0.8477	2.4752	2.8630
4	3.2785	0.9266	5.7451
5	3.3020	0.8838	5.7961
6	3.3020	0.0000	6.6799
cg	1.3333	0.2414	-

D_b = 5.0292
R_b = 2.5146
R_n = 6.0350
R_s = 0.2515
R_{as} = 0.0508

Dimensions in m

Figure 3. Orion Geometry [12].

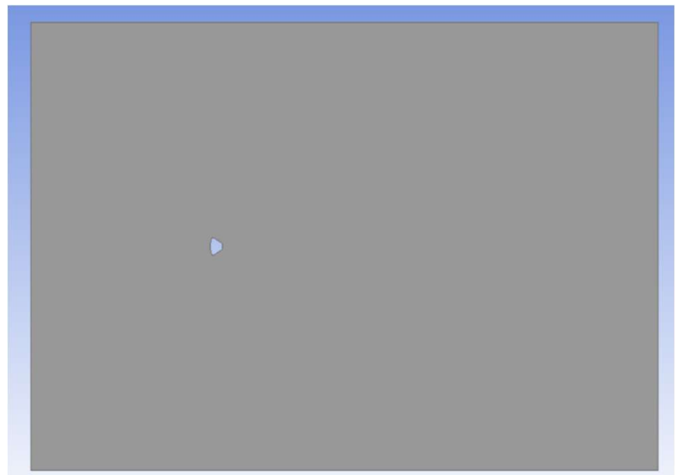

Figure 4. Initial Orion CFD Domain.

A simple mesh of the fluid domain was created with triangular elements, as shown in Fig. 5. To capture the complex interactions near the wall, the mesh size was decreased in the area of interest. The mesh's minimum orthogonal quality was 0.38, and the maximum aspect ratio was 4.3. Further boundary layer accuracy could be attained with an inflation layer around the capsule.

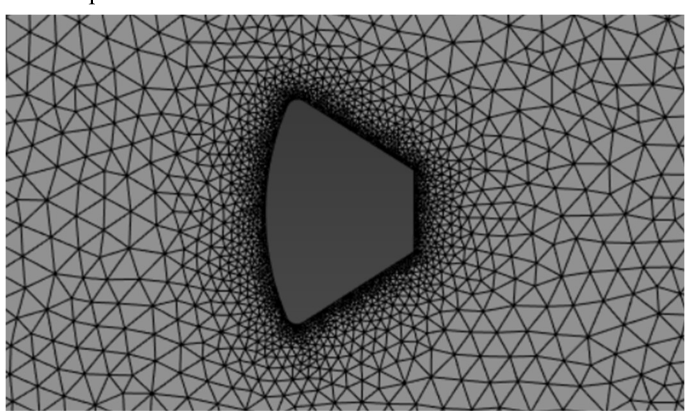

Figure 5. Initial Orion Triangular Mesh.

Solutions were completed with a transient, planar, density-based solver to account for the compressibility of the fluid. The farfield boundaries were given atmospheric values at an altitude of approximately 80 km with a speed of Mach 30, an angle of attack of $\alpha = 20°$, and a ratio of specific heats of $\gamma = 1.4$ for air, consistent with values from the Orion flights [13]. A laminar model was also used due to the extremely low density of air at this altitude. The solution was initialized using Standard Initialization computed from the farfield conditions.

Accurate characterization of the bow shock is of utmost importance in reentry simulations. For this reason, the main goal of initial simulations was to refine the shock through mesh adaptation and higher-order methods. The Mach contours for this solution case are shown in Fig. 6, and these contours reflect a Mach number of around 0.32 behind the normal shock, relatively consistent with analytical calculations at Mach 30, which predicted M = 0.38 from Eq. (2). Peak static temperatures in this condition were calculated to be in the range of 20,000 K. These values are not realistic, but they show the successful application of initial assumptions that do not allow dissociation of the fluid.

$$M^2 = \frac{1 + \frac{\gamma - 1}{2} M_\infty^2}{\gamma M_\infty^2 - \frac{\gamma - 1}{2}} \tag{2}$$

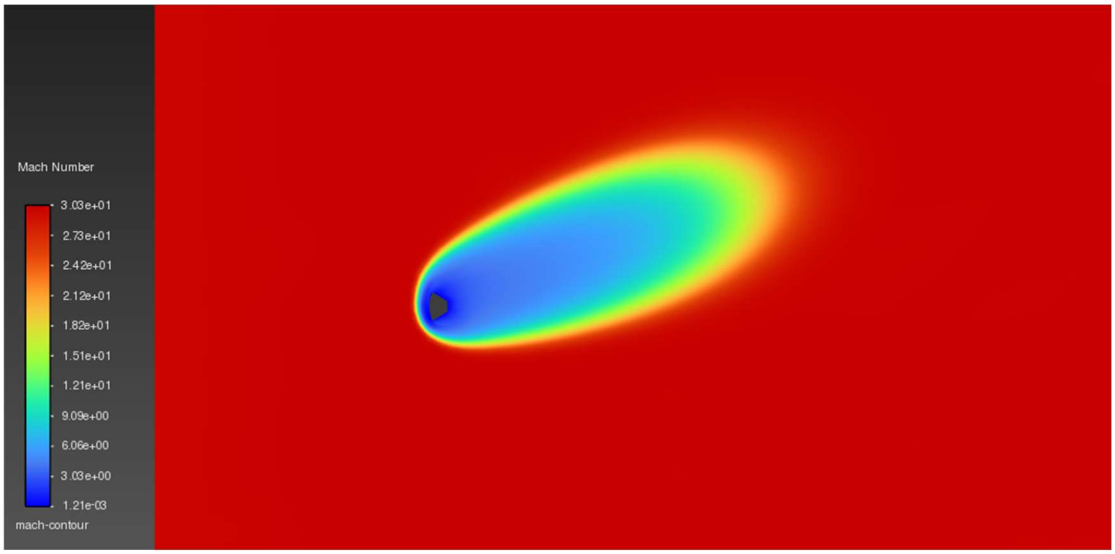

Figure 6. Mach Contour of Initial Orion Simulation

Progression of the solution was then made by turning on the Species Transport model with a 5-Species Air mixture, allowing for dissociation of the fluid. Temperature values predicted by this model decreased significantly, to around 14,900 K. This is an expected improvement, and yields temperatures closer to those expected at these speeds. Temperatures for the Apollo command module calculated by Anderson [14] were 11,600 K in Mach 32.5 flow at an altitude of 53 km. Our solution can further be refined by allowing for ionization of the fluid, with the 11-Species Air Mixture, and considering the possibility of a partial slip at the capsule wall. These changes should produce temperatures closer to the range expected and provide an excellent solution platform for transpiration cooling to be introduced into.

2. Transpiration Cooling on Flat Plate

Concurrently with the Orion reentry simulation, CFD simulations on simple cases for transpiration cooling have been conducted. The main goal of these analyses is to converge on an acceptable boundary condition for the porous media and observe proper mixing of the freestream fluid and the coolant along the wall. The fluid domain is shown in Fig. 7, with the wedge in the lower right corner serving as the porous wall through which coolant will be injected. The domain was meshed with triangular elements with an inflation layer along the wedge, as shown in Fig. 8.

Simple incompressible simulations have been run on these conditions with the wedge considered as a helium mass flow inlet. This is a vast simplification, but high enough mass flow rates can be specified so that mixing of the air and helium can be observed at distances that align closely with the boundary layer. Helium can also be specified at a much colder temperature than air, so the temperature change in the boundary layer can be verified as well. The contours for mass fraction of helium and temperature are shown in Fig. 9 and Fig. 10, respectively. While future simulations will much more accurately model temperature and pressure changes through the porous media and the boundary layer interaction between the coolant and freestream, these results represented a step towards those simulations with a simple and technically manageable first approach. Similarly, many simplified boundary conditions can be created that do not accurately preserve the wall properties of the heat shield and only consider some velocity or mass inlet into the domain. These low-fidelity conditions can show overall effectiveness at scale but cannot capture accurate particle mixing and surface interactions in the boundary layer.

Figure 7. Flat plate fluid domain.

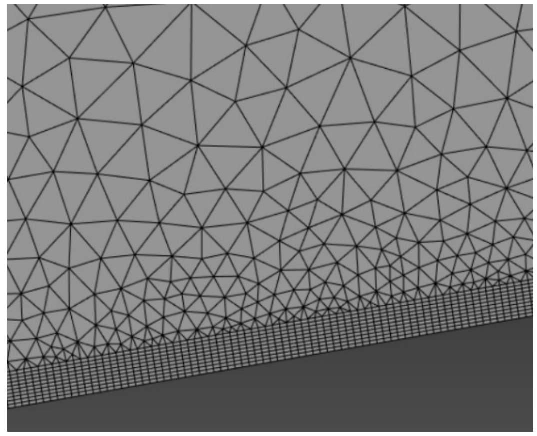

Figure 8. Flat plate triangular mesh with inflation layer.

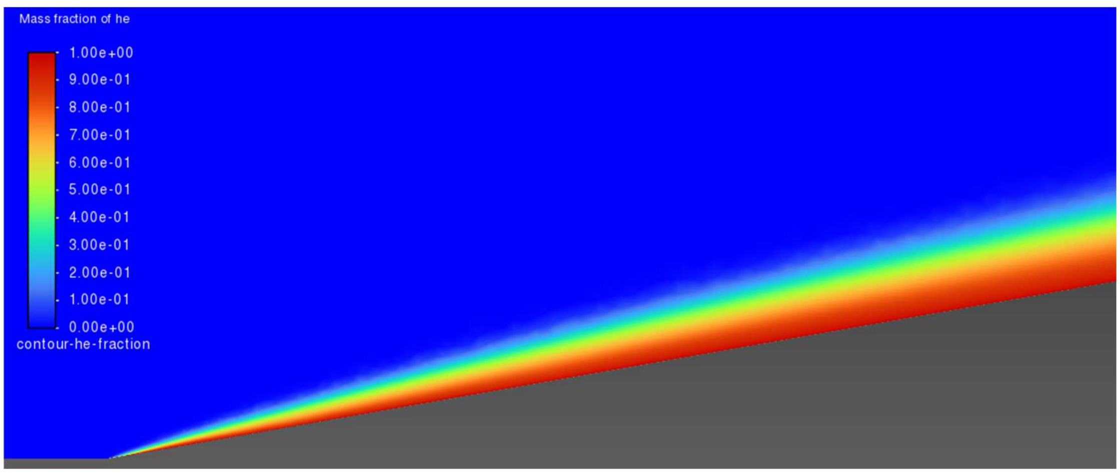

Figure 9. Mass fraction of helium contour for a flat plate with cold helium inlet.

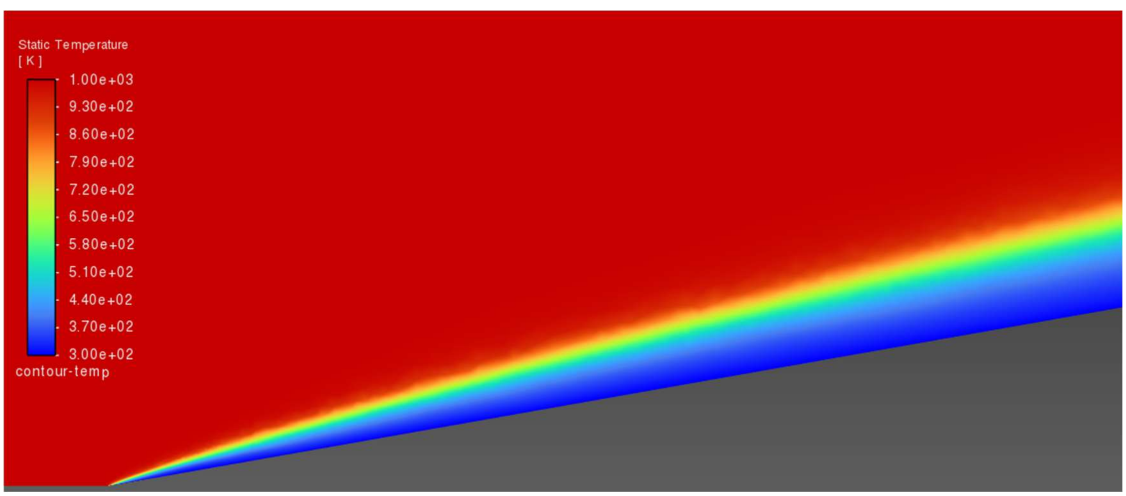

Figure 10. Static temperature contour for a flat plate with cold helium inlet.

3. Transpiration Cooling on a Section of Orion's Heat Shield

To begin a more accurate simulation of the porous wall at a small scale, a zoomed-in portion of the heat shield at the stagnation point was modeled in Ansys Fluent. This was modeled as a vertical flat plate with a thickness of t =

0.0254 m and a length of L = 0.05435 m where the helium will be injected through a simulated porous medium. The pressure-farfield inlet conditions were taken post-shock from the Orion reentry model at the wall, resulting in M = 0.32, T = 3000 K, Y_{O2} = 0.2288 kg/kg, Y_N = 0.0001812 kg/kg, and Y_{N2} = 0.7710 kg/kg. Using normal shock relations and the density of air at an altitude of 80 km, the post-shock gas density was ρ_g = 0.00011015 km/m^3. Rearranging Eq. (1) and implementing Eq. (3) results in Eq. (4), where the mass flux can be solved with a specified blowing ratio. Literature review of previous transpiration cooling research uses a moderate blowing ratio of F = 4% [8, 9].

$$u_\infty = M\sqrt{\gamma R_a T} \tag{3}$$

$$\dot{m} = F\rho_\infty M\sqrt{\gamma R_a T} \tag{4}$$

After performing the calculations, the coolant mass flux for a 4% blowing ratio is 0.001548 kg/s-m^2. For the simulation, the post-shock operating conditions were taken as a static pressure of 5400 Pa from the Orion simulation. The general setup of the transpiration cooling model used a density-based solver in steady flow. To maintain consistency with the original Orion model, the derived transpiration model used a laminar-viscous model. Figure 11 shows the geometry and meshing used in the CFD simulation. The mesh's minimum orthogonal quality was 0.99, and the maximum aspect ratio was 4.8 with a total of 16800 cells. The height of the geometry is 2 times the length of the plate, and the length is 0.2174 m.

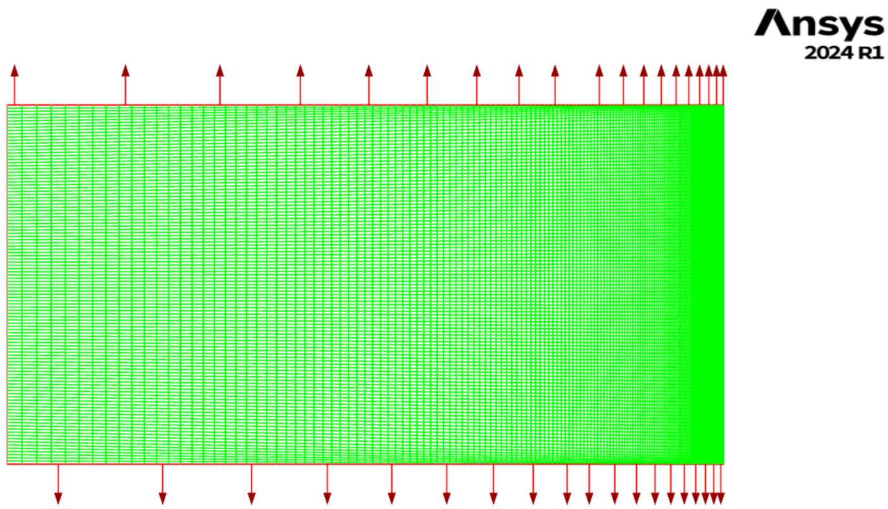

Figure 11. Meshing of the transpiration cooling model.

The left boundary was treated as a pressure-farfield, and the top and bottom boundaries were treated as pressure outlets. For the right boundary, a section of 0.05435 m was treated as the porous inlet. This section was in the middle of the right boundary, and was characterized by a uniform mass flux of ṁ = 0.001548 kg/s-m^2. It was given a wall thickness equal to t = 0.0254 m, and the temperature of the helium coolant was set to 273 K. The remaining portion of the right boundary (above and below the porous wall) was uncooled and thus treated as a wall with a temperature of 750 K taken from the Orion model. Solutions were obtained using an implicit formulation with a flux type of Roe-FDS, and the spatial discretization gradient was Least Squares Cell Based with a Second Order Upwind flow. Finally, the solution was initialized using a Hybrid Initialization.

C. Results

After running the simulation, a thin film of helium was observed over the wall, and this is shown in Fig. 12. The heat flux across the porous wall was computed to be 140 kW/m^2, and this represents a 95% cooling effectiveness from the 2 MW/m^2 heat flux measured across the Orion simulation wall. This mark is significantly greater than the theoretical and previously demonstrated cooling values of 65% [9] for transpiration cooling with a different geometry, and this can be attributed to simplifications in modeling the porous wall with different geometries and modeling software. The uniform mass flux boundary condition had a specified temperature equal to the stored temperature of the coolant, and this simplification could artificially boost cooling effectiveness by treating the full wall as being colder than in reality.

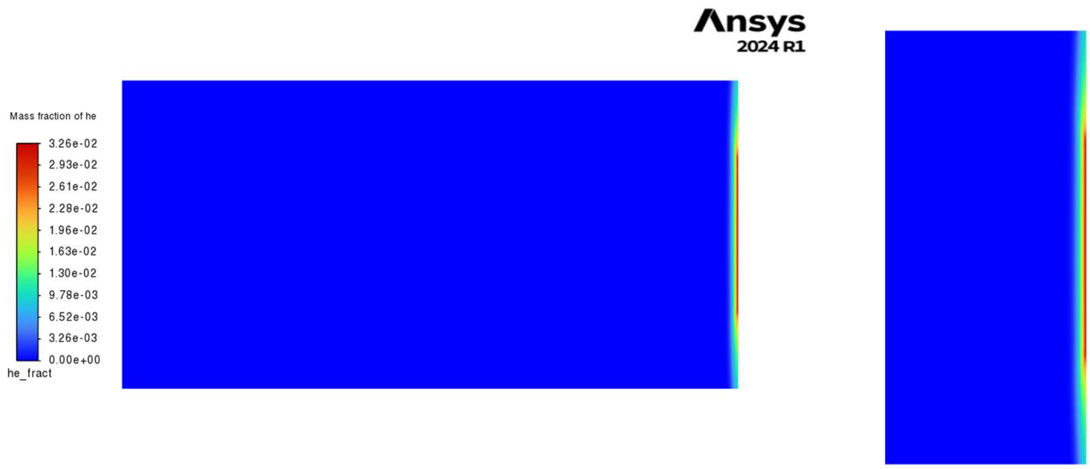

Figure 12. Mass fraction of helium results.

III. Future Work

Having selected the material and coolant to be used and developed a reentry simulation that can readily be used as a basis for comparison, work will immediately be made on increasingly accurate characterization of the porous medium. The proper boundary condition should allow the consideration of pressure losses through the porous medium and should consider cooling at the porous level instead of some uniform mass flux that cannot truly model interaction between the coolant and freestream. The Orion reentry simulation will be improved with further consideration of real gas effects where applicable to more closely replicate experimental results. A structural model should also be incorporated to enable the accurate determination of the heat shield's temperature for incorporation into the transpiration cooling model. In this way, any artificial increases in cooling effectiveness through wall temperature misrepresentation can be minimized.

IV. Conclusion

This study contributes a combined approach of material/coolant selection, CFD modeling, and data comparison to best validate an active transpiration cooling system used on a reusable reentry vehicle. In considering the most ideal cooling strategies for reusable vehicles, transpiration cooling can result in superior cooling efficiencies and reduced mass compared to other cooling methods, including ablatives, regenerative cooling, and film cooling. For the transpiration cooling system being analyzed, UHTC zirconium diboride (ZrB_2) was selected as the acting TPS and porous material for its porosity and high melting temperature, while helium was selected as the coolant for its increased cooling efficiency. The identification of the porous material and coolant provides a foundation for designing and assessing an integrated transpiration TPS. For the later inclusion of transpiration cooling in numerical analysis, a baseline 2D CFD case was initialized for the reentry of the Orion vehicle, and a 2D simulation was created to represent transpiration cooling over a flat plate with helium as the coolant. Initial flat plate results, although simplified, indicated significant cooling effects of helium-injected coolant on the boundary layer temperatures of the vehicle, with the 95% cooling effectiveness displaying the potential of transpiration cooling systems operating in hypersonic conditions. These simulations were intentionally kept simple to allow for the future implementation of advanced system features, such as porous media, multi-species injections, real-gas effects, and multiple inlet flows. While 2D simulations provide insight, improvements to 3D simulations would provide more accurate data through capturing more realistic effects experienced in reentry. This computational framework has laid the foundation for validating TPS predictions against currently existing Orion flight data. Overall, these findings support the feasibility of a lightweight, high-performing thermal active cooling solution. The methodology and results developed can be extended for designing an active cooling system that can be applied to future lunar missions, reentry from Mars expeditions, or hypersonic vehicles seeking optimized low-mass cooling solutions. Continued refinement of the model and current work will enable more accurate predictions and guide the development of a well-performing transpiration cooling system.

Acknowledgments

We would like to extend our gratitude to Dr. Bhushan of the Mississippi State Mechanical Engineering Department and Dr. Shinde of the Mississippi State Aerospace Engineering Department for their continuous support as our faculty advisors during this project. We would also like to thank the Mississippi State High Performance Computing Collaboratory.

References

[1] Miller, G.H., Haefling, J.A., "Improved Ablative Materials," *NASA*, Available: https://ntrs.nasa.gov/api/citations/19680018968/downloads/19680018968.pdf

[2] Mitchell, J.P., "Space Storable Regenerative Cooling Investigation," *NASA*, Available: https://ntrs.nasa.gov/api/citations/19710028084/downloads/19710028084.pdf

[3] Crawford, M.E., Choe, H., Kays, W.M., *et al*., "Full-Coverage Film Cooling Heat Transfer Study – Summary of Data for Normal-Hole Injection and 30° Slant-Hole Injection," *NASA*, Available: https://ntrs.nasa.gov/api/citations/19760011294/downloads/19760011294.pdf

[4] Rea, J., McNamara, L., Kane, M., "Orion Artemis I Entry Performance," *NASA*, Available: https://ntrs.nasa.gov/api/citations/20240000024/downloads/AAS_24_174_Orion_Artemis_I_Entry_Performance.pdf

[5] Peters, A.B., Zhang, D., Chen, S. *et al.,* "Materials design for hypersonics," *Nat Commun* 15, 3328 (2024). https://doi.org/10.1038/s41467-024-46753-3

[6] Reimer, T., Kuhn, M., Gulhan, A., Esser, B., Sippel, M., and Foreest, A., "Transpiration Cooling Tests of Porous CMC in Hypersonic Flow," AIAA Paper 2011-2251, April 2011, San Francisco, California.

[7] Zhang Q, Huang H, Lei C, Liu Y, Li W, "Review of Lightweight, High-Temperature Thermal Insulation Materials for Aerospace," *Materials*. 2025; 18(10):2383. https://doi.org/10.3390/ma18102383

[8] Hermann T., McGilvray M. and Naved I., "Performance of Transpiration-Cooled Heat Shields for Reentry Vehicles," AIAA Journal, Vol. 58, No. 2, 2020, pp. 830–841. https://doi.org/10.2514/1.J058515

[9] Naved I., Hermann T., and McGilvray M., "Numerical Simulation of Transpiration Cooling for a High-Speed Vehicle with Substructure," AIAA Journal, Vol. 59, No. 8, 2021, pp. 3043–3053. https://doi.org/10.2514/1.J059771

[10] Liu, Y., Jiang, P., Jin, S., Sun, J., "Transpiration cooling of a nose cone by various foreign gases," *International Journal of Heat and Mass Transfer*, Vol. 53, No. 23, 2010, pp. 5364-5372. https://doi.org/10.1016/j.ijheatmasstransfer.2010.07.019

[11] Hall, N., "Real gas effects," *NASA* Available: https://www.grc.nasa.gov/WWW/BGH/realgas.html.

[12] Votta, R., "Hypersonic high altitude aerothermodynamics of a space re-entry vehicle - sciencedirect," *Aerospace Science and Technology* Available: https://www.sciencedirect.com/science/article/abs/pii/S1270963812000247.

[13] Tigges, M. A., "Orion Capsule Handling Qualities for Atmospheric Entry," *NASA* Available: https://ntrs.nasa.gov/api/citations/20110013203/downloads/20110013203.pdf.

[14] Anderson, J. D., *High temperature gas dynamics an introduction for physicists and Engineers*, Cham: Springer International Publishing, 2014.